

Supplementary Information-Modeling tumor transport and growth with poroelastic biopolymer networks

Zecheng Li^{1,a}, Yifei Ren^{2,3,a}, Sharvari Kemkar^{4,3,a}, Paul Mollenkopf⁵, Jakub Kochanowski¹,
Paul A. Janmey^{1,5}, Prashant K. Purohit^{2,3}, Ravi Radhakrishnan^{1,3,b}, and Kyle H. Vining^{6,7,8,c}

¹*Department of Bioengineering, School of Engineering and Applied Science, University of Pennsylvania, Pennsylvania,
19104, United States*

²*Department of Mechanical Engineering and Applied Mechanics, School of Engineering and Applied Science, University
of Pennsylvania, Pennsylvania, 19104, United States*

³*Penn Institute for Computational Science, University of Pennsylvania, Pennsylvania, 19104, United States*

⁴*Department of Chemical and Biomolecular Engineering, School of Engineering and Applied Science, University of
Pennsylvania, Pennsylvania, 19104, United States*

⁵*Department of Physiology, School of Medicine, University of Pennsylvania, Pennsylvania, 19104, United States*

⁶*Department of Preventive and Restorative Sciences, School of Dental Medicine, University of Pennsylvania,
Pennsylvania, 19104, United States*

⁷*Department of Materials Science and Engineering, School of Engineering and Applied Science, University of
Pennsylvania, Pennsylvania, 19104, United States*

⁸*Center for Innovation and Precision Dentistry, University of Pennsylvania, Pennsylvania, 19104, United States*

^aThese authors contributed equally to this work.

^bElectronic mail: rradhak@seas.upenn.edu

^cElectronic mail: viningk@upenn.edu

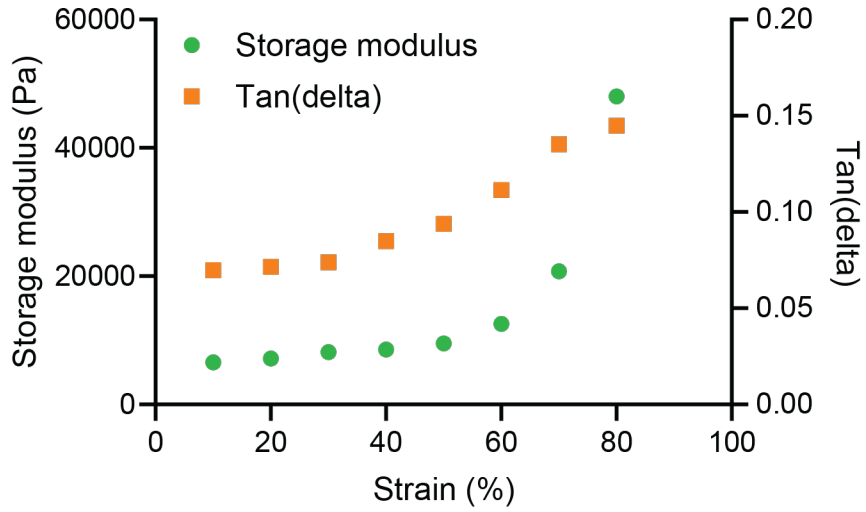


Fig. 1. Storage moduli and $\tan(\delta)$ as a function of compressive strain for ionic Alg under slow stepwise compressions (strain rate 0.025%/s), where storage moduli and $\tan(\delta)$ are measured when the stress is fully relaxed.

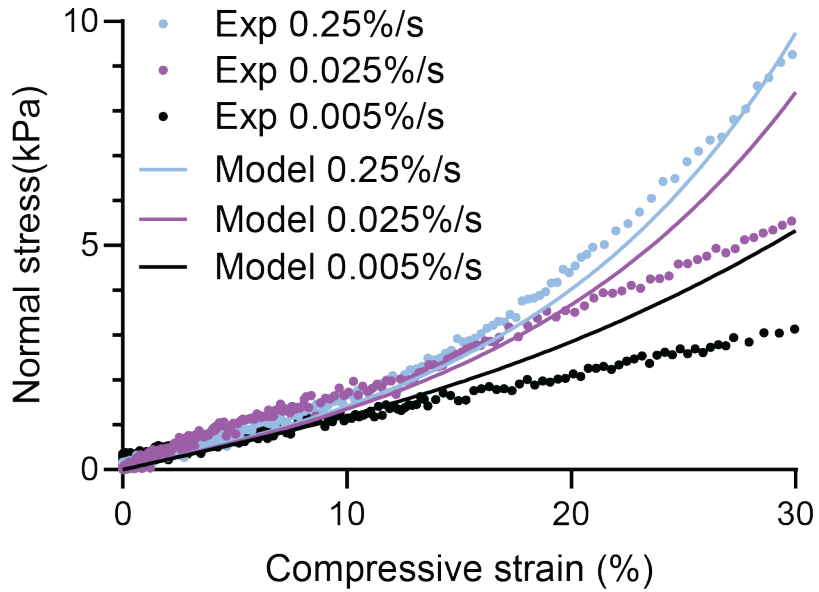


Fig. 2. Normal stress vs. compressive strain under various strain rates from experiments and FEM simulations.

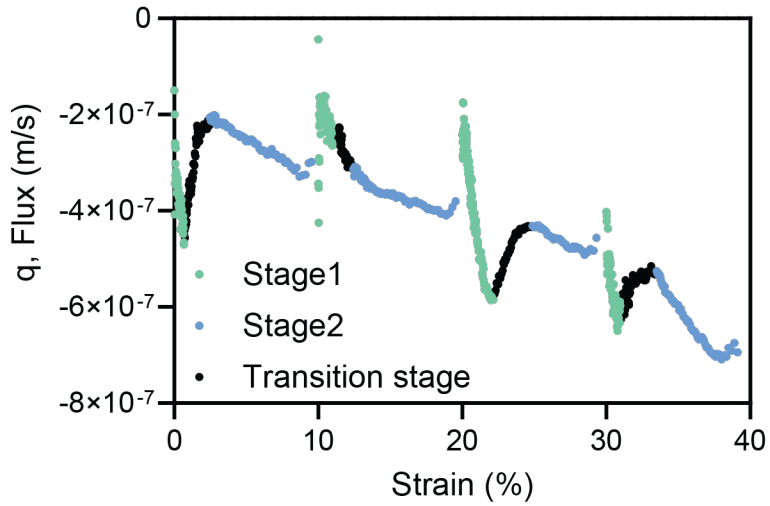


Fig. 3. Fluid flux vs. strain under stepwise compression, which repeatedly generated stage 1's fast-decreasing regions and the transition stage from stage 1 to stage 2.

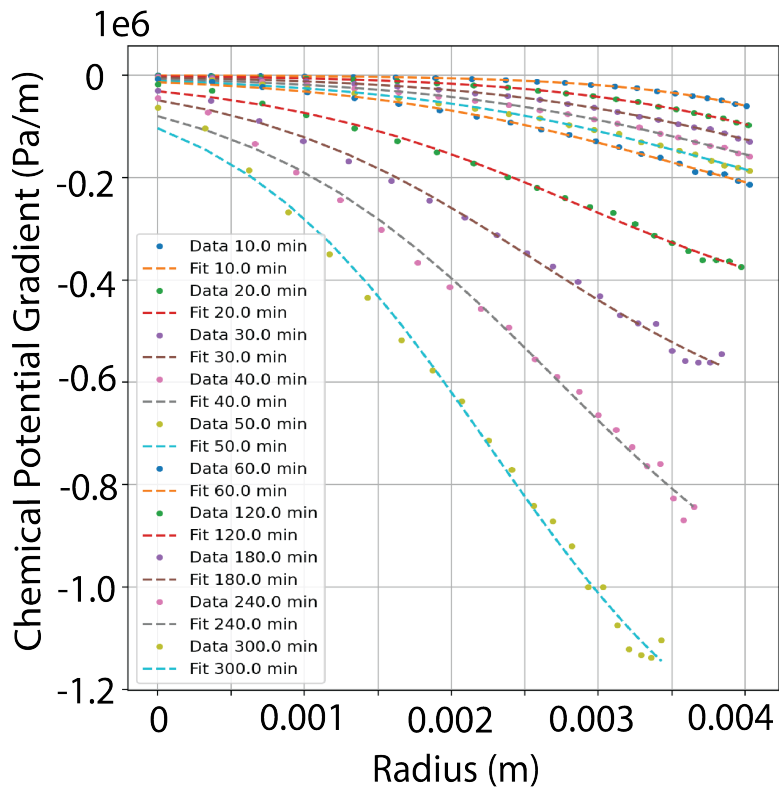


Fig. 4. 30 % compression in 5 hrs. The radial chemical potential gradient profiles were obtained from the FEM simulation results. This data was recorded at discrete times ($t=10, 20, 30, 40, 50, 60, 120, 180, 240, 300$ min) throughout the simulation. Logistic function was fit to radial chemical potential gradient profiles for all these time points. The gradients are relatively flat in radial direction at the initial time points. They become steeper as the simulation progresses.

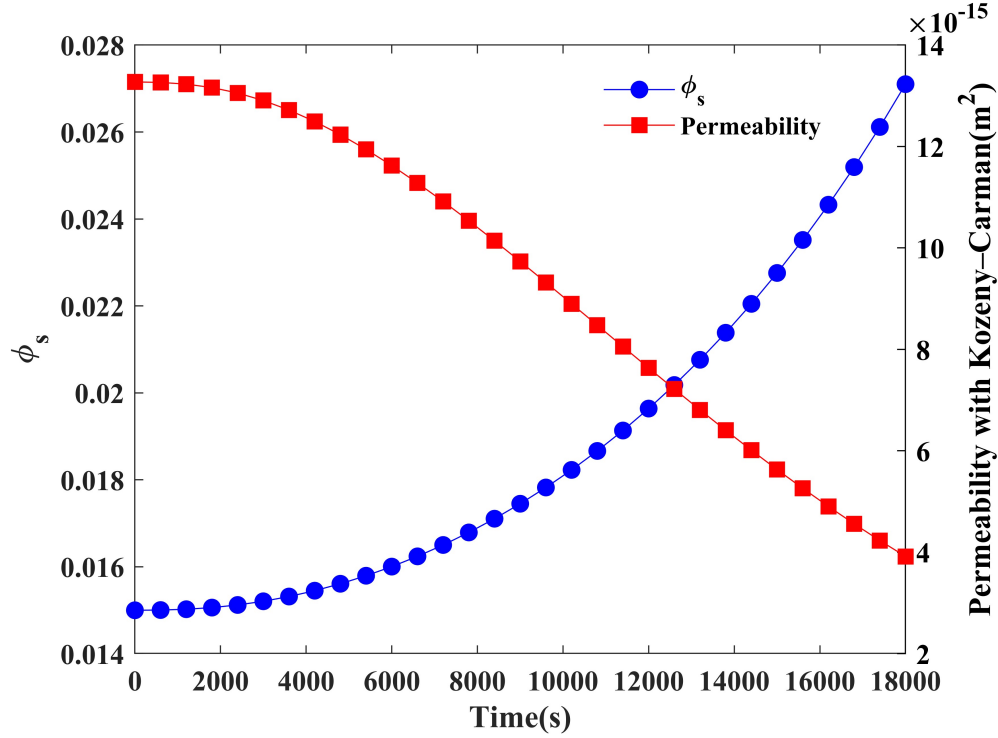


Fig. 5. Solid volume fraction and permeability values for the simulation lattice as a function of time, which is obtained by 30% compression in 5 hrs.

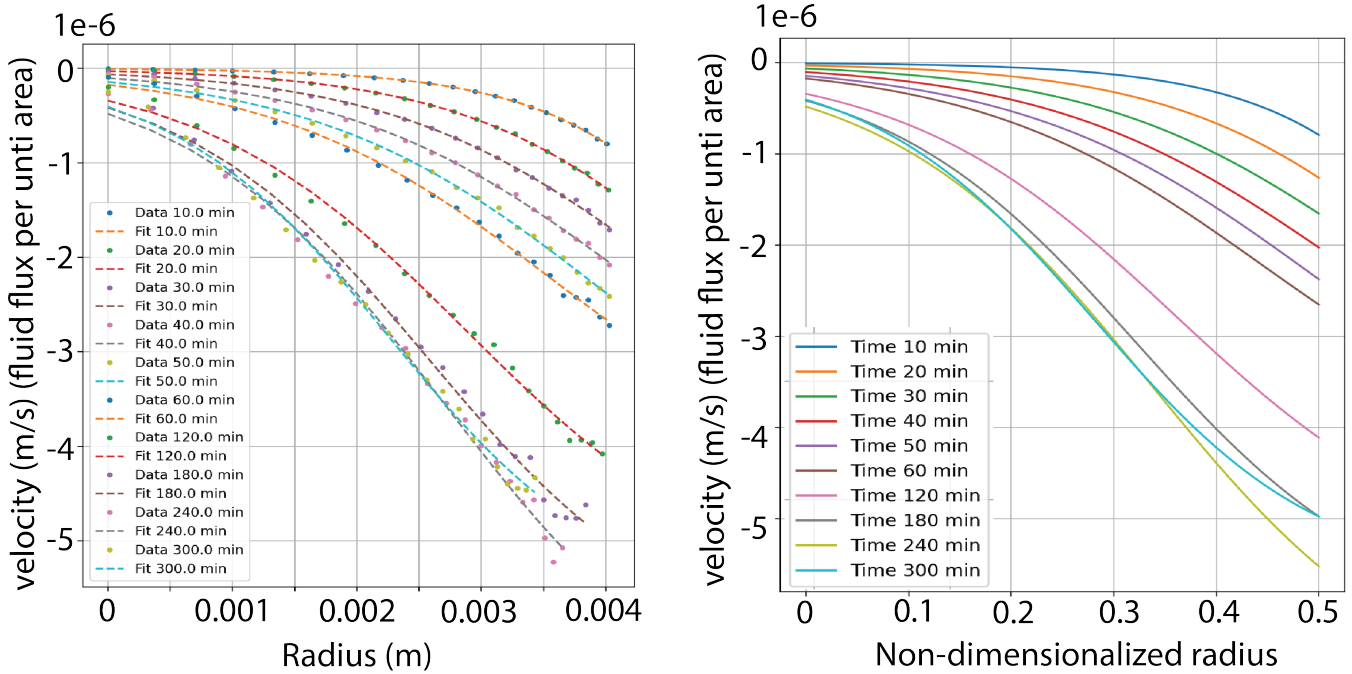


Fig. 6. Velocity is calculated as a product of chemical potential gradient and mobility. The first plot (left) shows the velocity profile (function of radius and time) as a function of time. The second plot (right) shows the mapped velocity profiles onto the non-dimensionalized radius for the advection-diffusion PDE setup.

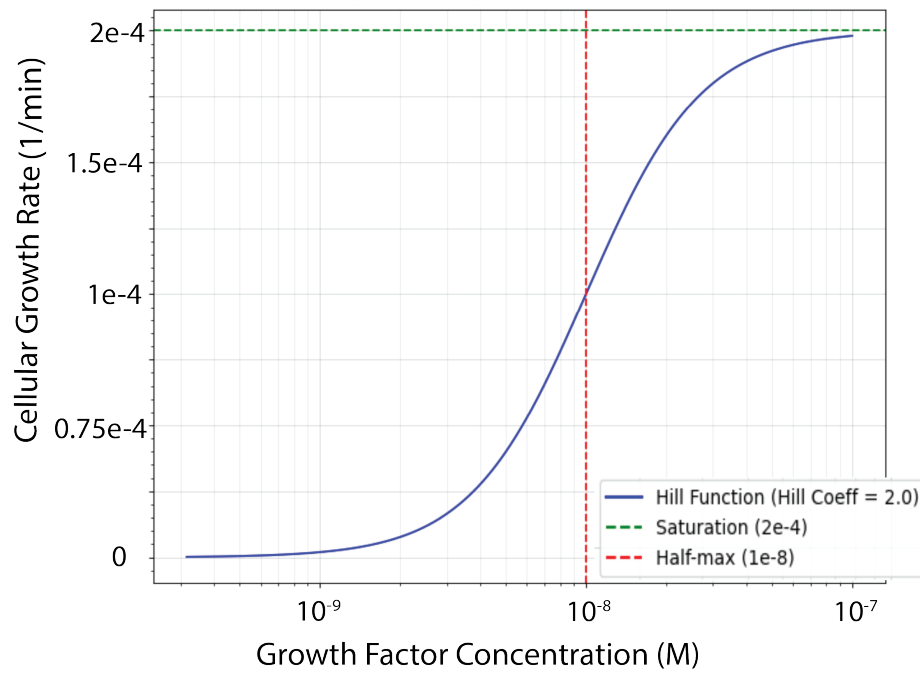


Fig. 7. The cellular proliferation rule in the ABM was set as a sigmoidal function of local growth factor concentration.

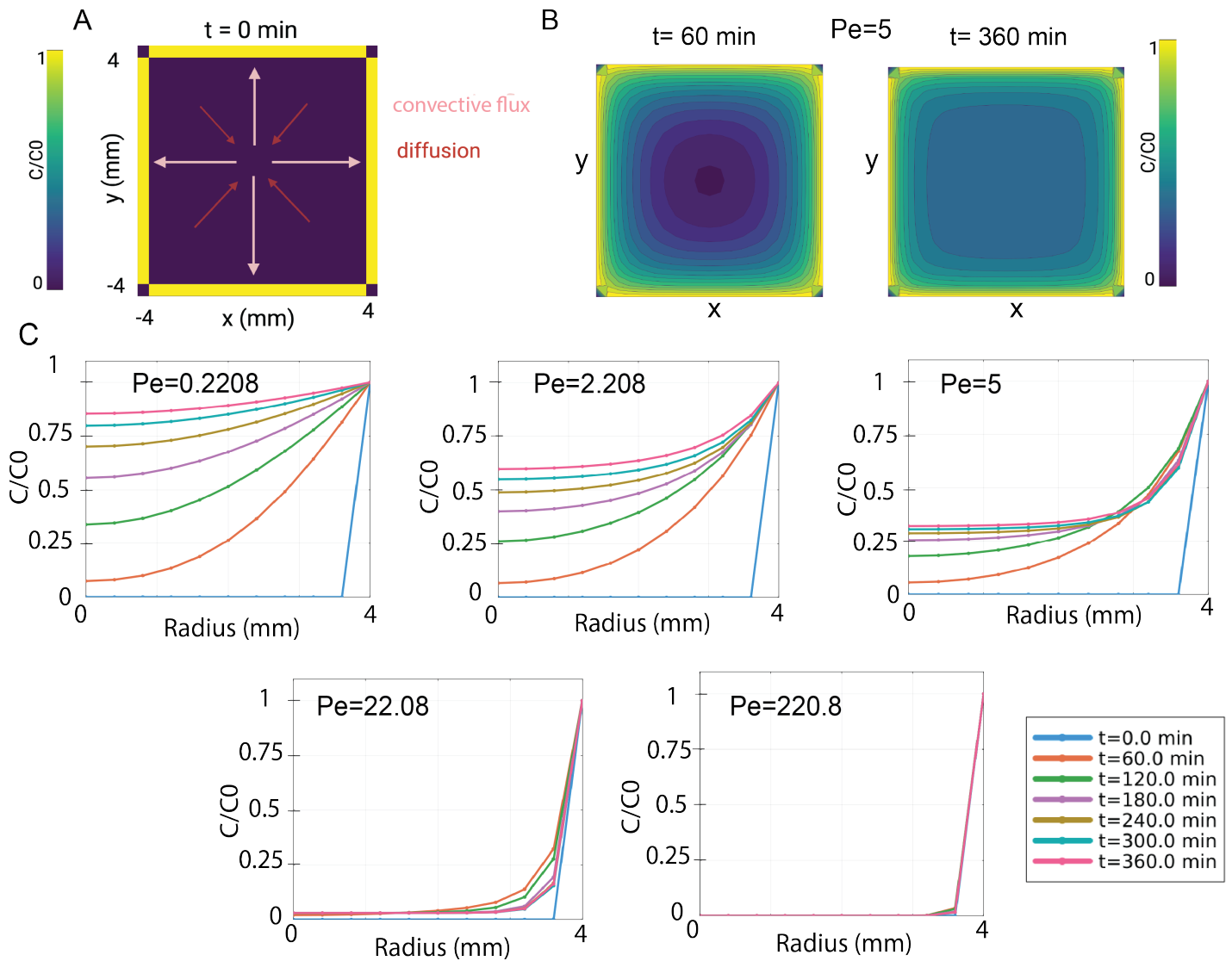


Fig. 8. Influence of Péclet number on growth-factor distribution - Simulations initialized from a Growth Factor Depleted Lattice. A) At $t=0\text{ min}$, the concentration field is 0 across the $8\text{ mm} \times 8\text{ mm}$ domain and boundary conditions are set to 1. Pink arrows indicate the imposed outward convective flux, while red arrows show the inward direction of diffusion. B.) Two-dimensional concentration contours at $t=0\text{ min}$ (left) and $t=360$ (right) illustrate how the initially depleted field evolves under a moderate flow regime (here, $Pe = 5.0$). By 360 min, a nearly square-shaped plateau of low concentration persists in the interior, bounded by steep boundary layers. C.) Radial profiles of C/C_0 at six time points (0, 60, 120, 180, 240, 360 min) for five Péclet numbers (0.2208, 2.208, 5.0, 22.08, 220.8). At low Pe , diffusion dominates and enables a significant influx of growth factors. As Pe increases, convective transport limits this inward flux and confines accumulation to narrow boundary regions.

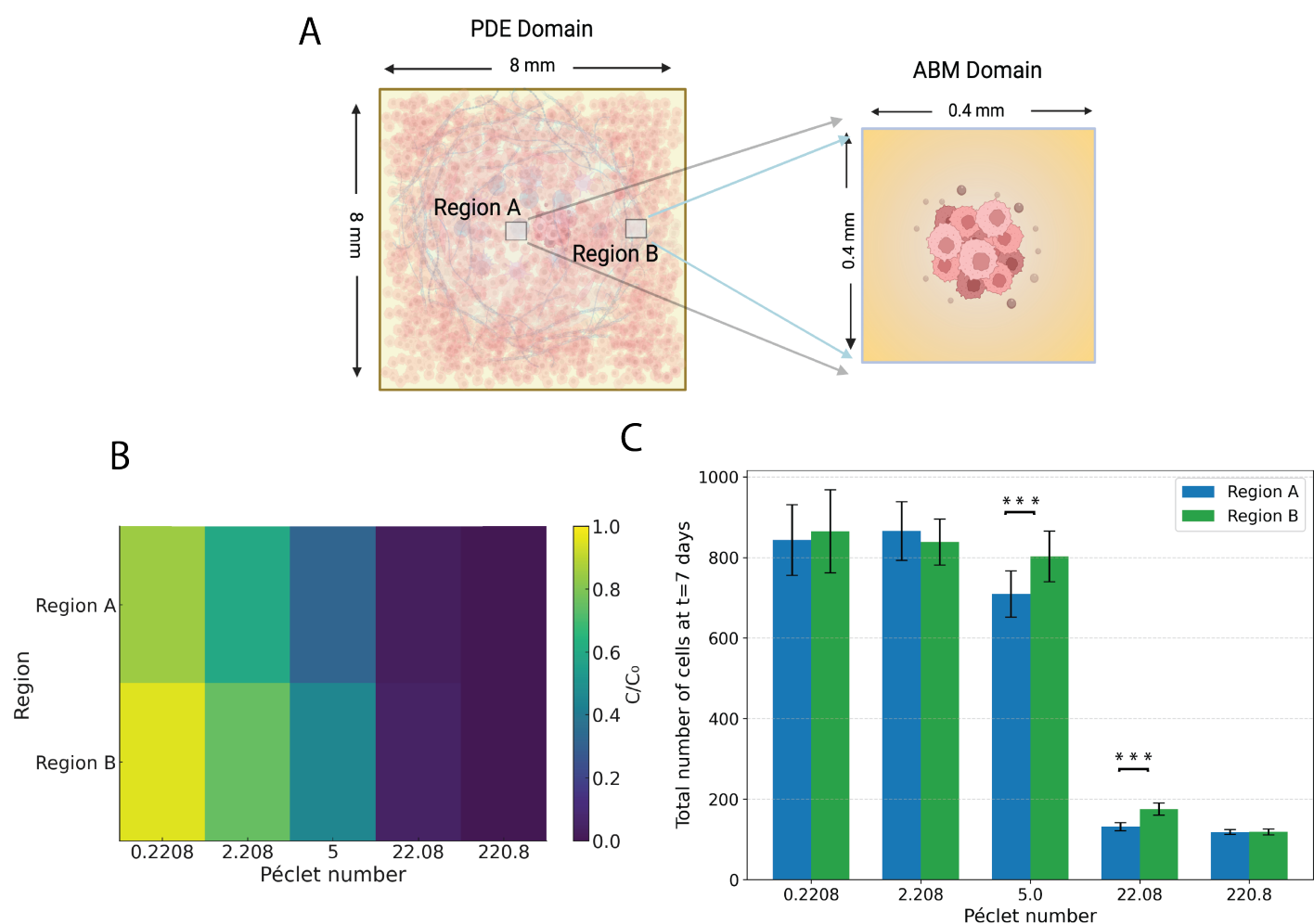


Fig. 9. Coupling growth factor transport and tumor growth results across scales A) Setup of the computational study - PDE domain on the $8\text{ mm} \times 8\text{ mm}$ lattice and tumor growth ABM domain on $0.4\text{ mm} \times 0.4\text{ mm}$ regions of the lattice. B) Heatmap - summarizing the Region A and Region B growth factor (GF) concentrations (at $t=6$ hrs). Spatial heterogeneity in growth factor availability between Regions A and B reduces as Pe increases. C) Tumor load at $t = 7$ days / 10080 min) at Regions A and B, under different Pe . At intermediate Pe values, tumor growth differs significant between regions A and B. Tumor load bars show the $\mu \pm \sigma$ from ten independent ABM stochastic runs per condition. Welch's two-sample t-test was applied to each Region A-B pair; an asterisk indicates a significant difference. ($p < 0.01$) and three asterisks indicate $p < 0.0001$.

Parameter Description	Value	Unit
Total simulation time	7200	min
Domain size in x-direction	400	μm
Domain size in y-direction	400	μm
Grid resolution (dx, dy)	20	μm
Initial number of cells (t=0)	200	cells
GF diffusion coefficient	100	$\mu\text{m}^2/\text{s}$
GF decay rate	0	1/min
GF initial condition	GF concentration from PDE solution	M
GF Dirichlet BC	GF concentration from PDE solution	M
Cell proliferation rate	$0-2 \times 10^{-4}$ (sigmoid function)	1/min
Cell apoptosis rate	5.3×10^{-5}	1/min

Table 1. Summary of ABM (PhysiCell) parameters used to generate a family of tumor growth curves from the agent based simulations.

Parameter Description	Value	Unit
Radius of the alginate gel r	4	mm
Thickness of the alginate gel t	2	mm
Reference solid volume fraction ϕ_s^{ref}	0.015	
Small strain shear modulus G_1	$4000/\phi_s^{\text{ref}}$	Pa
Shear modulus related to large deformation G_2	$700000/\phi_s^{\text{ref}}$	Pa
Initial osmotic pressure π_0	3000	Pa
Power law coefficient β_1	1.02	

Table 2. Summary of finite element parameters used to simulate the compression of alginate gels.